Role of hydrogen in surface reconstructions and growth of GaN

Chris G. Van de Walle[a)]
Palo Alto Research Center, 3333 Coyote Hill Road, Palo Alto, California 94304, Fritz-Haber-Institut der Max-Planck-Gesellschaft, Faradayweg 4-6, D-14 195 Berlin-Dahlem, Germany, and Paul-Drude-Institut, Hausvogteiplatz 5-7, D-10117 Berlin, Germany

J. Neugebauer
Fritz-Haber-Institut der Max-Planck-Gesellschaft, Faradayweg 4-6, D-14 195 Berlin-Dahlem, Germany

(Received 24 January 2002; accepted 21 April 2002)

We present first-principles calculations for the atomic structure and energetics of hydrogenated GaN(0001) surfaces. The geometry of the most relevant surface reconstructions is discussed in detail. Finite-temperature effects are included through calculations of the Gibbs free energy and the stability of various surface reconstructions is analyzed in terms of a generalized surface phase diagram. A comparison with recent experiments elucidates the energetic and structural properties of GaN surfaces under growth conditions. © *2002 American Vacuum Society.*
[DOI: 10.1116/1.1491545]

I. INTRODUCTION

Knowledge of surface reconstructions on nitride semiconductors is important for improved control over growth, materials properties, and interface formation. Most of the investigations to date, both theoretical and experimental, have focused on *bare* GaN surfaces. Previous computational studies of GaN surfaces include investigations of cubic surfaces[1–6] and of the nonpolar surfaces of wurtzite GaN.[1,5,7] The technologically most relevant (0001) surface of GaN was studied in Refs. 8–11.

Our present work goes beyond these studies in two respects. First, we include interactions between hydrogen and the surface, and second, we address finite-temperature effects. The first point is important because hydrogen is present in high concentrations in the most commonly used growth techniques for nitride semiconductors, including metalorganic chemical vapor deposition (MOCVD) and hydride vapor-phase epitaxy. Even in molecular-beam epitaxy (MBE) hydrogen has been introduced, either from a plasma source or through growth with a NH_3 source. Hydrogen has also been observed to have important effects on the growth of GaN. For instance, Yu *et al.*[12] observed that the introduction of H during MBE growth of GaN using a rf plasma source can increase the growth rate by as much as a factor of 2. Hydrogen was also reported to improve the crystal quality of GaN in rf-MBE.[13] As to the second point, the development of a finite-temperature formalism is essential if we want our results to be relevant for growth of GaN, which is carried out at temperatures around 1000 °C. This will require the evaluation of *Gibbs free energies*.

Some previous computational studies have actually addressed adsorbates on GaN surfaces, without explicitly including the temperature dependence: Bungaro *et al.*[14] studied Mg on GaN(0001), Picozzi *et al.*[15] investigated Al on zincblende GaN, Neugebauer *et al.*[2] looked at As on GaN(001), and Zywietz *et al.* addressed oxygen on wurtzite GaN,[16] as well as diffusion of Ga and N adatoms on GaN(0001) and GaN($000\overline{1}$).[17] Only a very limited amount of work has been devoted to hydrogen, however: Northrup *et al.*[18] examined H on GaN($10\overline{1}0$), and the studies of Fritsch *et al.*[11] and Rapcewicz *et al.*[8] included a result for a specific hydrogen-terminated (0001) surface, with 3/4 monolayer (ML) of H. The work of Elsner *et al.*[19] also included a 1/2 ML coverage (which we find to be unstable).

Experimental investigations of hydrogen of GaN surfaces are also rare: besides the growth studies mentioned above, Sung *et al.*[20] investigated MOCVD-grown GaN using time-of-flight scattering and recoiling spectrometry, and inferred the presence of hydrogen on the surface. Hydrogen desorption was studied by Chiang *et al.*[21] and by Shekhar and Jensen.[22] Bellitto *et al.*,[23] finally, applied a variety of experimental probes, including high-resolution electron energy loss spectroscopy, to the study of intentionally hydrogenated GaN surfaces.

Our first-principles calculations, based on pseudopotential-density-functional theory, allow us to investigate the stability of surface reconstructions as a function of stoichiometry (Ga-rich versus N-rich conditions), as well as of the abundance of hydrogen in the growth environment. We focus here on the GaN(0001) surface, which is technologically most relevant: indeed, this is the polarity observed for MOCVD growth of GaN on sapphire, as well as for MBE of GaN on Si-face SiC. At $T=0$, we find that reconstructions maximizing the number of N–H bonds are favored, due to the large N–H bond strength. Growth occurs at elevated temperatures, however, and therefore we have extended the formalism to include vibrational, rotational, and translational energies and entropies. Inspection of the Gibbs free energies at temperatures relevant for growth produces a picture that is very different from the $T=0$ results. Nitrogen-rich conditions still favor N–H bonds, but moving towards Ga-rich conditions we find that 2×2 reconstructions involving only Ga–H bonds (3/4 ML H coverage), or even hydrogen-free

---

[a)] Electronic mail: vandewalle@parc.xerox.com

surfaces (Ga adatom or Ga bilayer reconstructions) are more stable.

Changes in temperature and pressure strongly affect the relative stability of various reconstructions; such information is best presented in a phase diagram, but due to the large number of degrees of freedom a traditional phase diagram would be difficult to analyze or visualize. We have been able to show that the number of degrees of freedom can be reduced to two if *chemical potentials* are chosen as the variables.[24] The resulting generalized surface phase diagram provides immediate insight into the stability of various surface structures as a function of growth conditions.

Experimental studies of the surface structure at high temperature in the presence of gases (as relevant for MOCVD) are exceedingly difficult. We are fortunate that a set of experimental studies has been performed by Munkholm *et al.*[25,26] based on grazing incidence x-ray scattering. Their *in situ* observations of surface reconstructions in a MOCVD growth environment can be directly linked to our theoretical results. The experimentally measured transition between two reconstructions turns out to coincide with a specific boundary in our phase diagram, offering valuable information about the nature of the observed structures.

Some of our results have been discussed in Ref. 24. In this article we will provide additional details about the geometry of the surface reconstructions, and about the comparison with experiment.

Section II briefly describes the computational approach. Sections III and IV discuss the atomic and electronic structure of the surface reconstructions, and Sec. V addresses the comparison with experiment. Section VI concludes the article.

II. METHODS

The first-principles calculations are based on density-functional theory in the local-density approximation,[27] using *ab initio* pseudopotentials, implemented in an optimized code.[28] For hydrogen we use the Coulomb potential. The Ga $3d$ states are explicitly included as valence states, requiring a 70 Ry plane-wave cutoff. We use a slab geometry, consisting of at least four double layers of GaN plus at least 7 Å of vacuum. The lower surface of the slab is passivated with fractionally charged hydrogen atoms, and the positions of all atoms in the lower half of the slab are kept fixed, allowing us to accurately determine energy differences between surface reconstructions on the upper surface of the slab. A $2\times2\times1$ Monkhorst–Pack mesh[29] was used in the calculations with 2×2 and $\sqrt{3}\times\sqrt{3}$ periodicity. Convergence tests indicated that these choices allow us to determine energy differences to an accuracy of better than 0.05 eV. Our calculated lattice constant for GaN is $a=3.195$ Å, essentially the same as the experimental value.

We define the *Gibbs free energy of formation* of a particular surface reconstruction as the free-energy difference between the reconstructed surface and a reference surface, for which we choose the ideal, bare 1×1 surface (relaxed but unreconstructed):

$$\Delta G^f = E_{\mathrm{tot}}[\mathrm{GaN}(0001)] - E_{\mathrm{tot}}[\mathrm{GaN}(0001),\ \mathrm{ideal}] + \Delta F_{\mathrm{vib}} - n_{\mathrm{Ga}}\mu_{\mathrm{Ga}} - \mu_{\mathrm{N}}\mu_{\mathrm{N}} - n_{\mathrm{H}}\mu_{\mathrm{H}}. \tag{1}$$

$E_{\mathrm{tot}}[\mathrm{GaN}(0001)]$ is the calculated total energy for the surface under study, and $E_{\mathrm{tot}}[\mathrm{GaN}(0001),\ \mathrm{ideal}]$ is the total energy of our reference system. $n_{\mathrm{Ga(N,H)}}$ is the number of Ga(N,H) atoms that is added to the unit cell (positive or negative). The term ΔF_{vib} includes vibrational contributions to the free energy, and is discussed below. μ_{Ga} and μ_{N} are the chemical potentials of Ga and N, i.e., the free energies of the reservoirs with which Ga and N atoms are exchanged. In equilibrium, $\mu_{\mathrm{Ga}}+\mu_{\mathrm{N}}=E_{\mathrm{tot}}[\mathrm{GaN}]$, i.e., the total energy of a two-atom unit of bulk GaN, calculated for the structurally optimized wurtzite structure. This leaves us, in effect, with a single parameter to describe the stoichiometry, for which we will choose μ_{Ga}. Ga-rich conditions place an upper limit on μ_{Ga}, given by $\mu_{\mathrm{Ga[bulk]}}$; N-rich conditions place an upper limit on μ_{N}, given by $\mu_{\mathrm{N[N_2]}}$, yielding a lower limit on μ_{Ga}. The total energy of GaN can also be expressed as $E_{\mathrm{tot}}[\mathrm{GaN}]=\mu_{\mathrm{Ga[bulk]}}+\mu_{\mathrm{N[N_2]}}+\Delta H_f[\mathrm{GaN}]$, where $\Delta H_f[\mathrm{GaN}]$ is the enthalpy of formation (negative for a stable compound). μ_{Ga} thus varies over a range corresponding to the magnitude of the enthalpy of formation of GaN. Our calculated value for $\Delta H_f[\mathrm{GaN}]$ is -1.24 eV (experiment: -1.17 eV).[30] Our use of an equilibrium formalism for the chemical potentials is justified by the fact that in MOCVD growth the conditions are usually close enough to equilibrium (as established by sufficiently high mobilities of point defects on the surface and in the bulk) for this assumption to be valid.

The chemical potential of hydrogen μ_{H} is a free parameter describing the abundance of hydrogen in the environment. This chemical potential is given by the free energy of H_2, assuming that there are no kinetic barriers to equilibration with H_2; experiments have shown this to be true above 600 °C.[21]

Now we discuss how finite-temperature effects are incorporated into the formation energy defined in Eq. (1). The temperature dependence of the hydrogen chemical potential is given by

$$2\mu_{\mathrm{H}} = E_{\mathrm{H_2}} + kT\ln\left(\frac{pV_Q}{kT}\right) - kT\ln Z_{\mathrm{tot}} - kT\ln Z_{\mathrm{vib}}, \tag{2}$$

where $E_{\mathrm{H_2}}$ is the energy of an H_2 molecule, k is the Boltzmann constant, T is the temperature, and p is the pressure. $V_Q=(h^2/2\pi mkT)^{3/2}$ is the quantum volume, and Z_{rot} and Z_{vib} are the rotational and vibrational partition functions.

The term ΔF_{vib} in Eq. (1) describes the difference in vibrational free energies between the surface under study and our reference system (the ideal bare surface). The temperature dependence arises from vibrational contributions to the energy and entropy and could, in principle, be evaluated entirely from first principles based on a calculation of the vibrational spectrum. This would, however, be a tedious exercise, to be repeated for each of the surface reconstructions under study. Inspection of the vibrational modes calculated for a subset of structures reveals that, to a very good approxi-

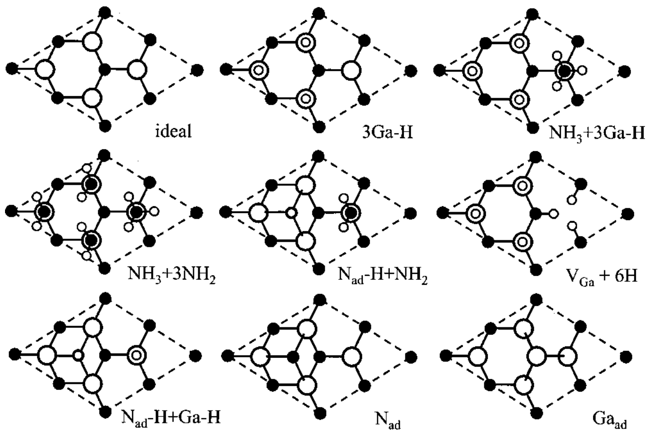

FIG. 1. Schematic top view of prevalent 2×2 reconstructions for GaN(0001) surfaces. Large white circles represent Ga atoms, black circles N, and small white circles H.

mation, the vibrational free energy for a given reconstruction can be calculated by assuming specific frequencies for the relevant vibrational modes of the bonds that appear in these surface reconstructions, i.e., we assume the vibrational modes only depend on the atoms (or molecular units) directly involved in the bond, and are otherwise independent of the environment. We estimate that vibrational frequencies would not change by more than $\pm 100\ \mathrm{cm}^{-1}$ due to changes in the environment, yielding a conservative error bar of less than 0.1 eV on the free energies calculated using this approximation. We have used the following vibrational frequencies:[18] for Ga–H, 2010 cm^{-1} (250 meV) for stretching and 990 cm^{-1} (123 meV) for bending; for N–H, 3450 cm^{-1} (429 meV) for stretching and 1020 cm^{-1} (127 meV) for bending; for adsorbed NH_3, in addition to the stretching and bending modes above, two modes at 1691 cm^{-1} (210 meV), and a Ga–NH_3 torsion mode at 240 cm^{-1} (30 meV); and for adsorbed NH_2, in addition to the stretching and bending modes above, a scissors mode at 1450 cm^{-1} (180 meV) and a Ga–NH_2 torsion mode at 240 cm^{-1} (30 meV). The vibrational free energy is then given by summing over the modes with frequency ω_i:

$$F_{\mathrm{vib}}=\sum_i \frac{\hbar\omega_i}{2}+kT\sum \ln[1-e^{-(\hbar\omega_i/kT)}], \tag{3}$$

where the first term is the zero-point energy.

III. ATOMIC STRUCTURE

In the course of our investigations, we examined over 30 different surface reconstructions, including structures with 1×1, 2×2, and $\sqrt{3}\times\sqrt{3}$ periodicity. Although we made no *a priori* assumptions, we find *a posteriori* that the lowest-energy structures all exhibit 2×2 symmetry; this result is related to the *electron counting rule*, which will be discussed in Sec. IV.

Figure 1 schematically depicts those reconstructions that will turn out to be most relevant. In the absence of hydrogen, we find the lowest energy structures to be those previously reported for bare GaN(0001);[10] specifically, under Ga-rich conditions the most favorable reconstruction is the Ga adatom in a $T4$ position (i.e., above a second-layer N atom), while under N-rich conditions the N adatom in the $H3$ position (i.e., the "hollow site" above the hexagonal channel) is most stable. Under extreme Ga-rich conditions a Ga-bilayer reconstruction is energetically most favorable.[31]

In the presence of hydrogen, the equilibrium structure that is dominant at $T=0$ is the NH_3+3NH_2 reconstruction. It consists of adding one NH_3 and three NH_2 molecules in on-top positions (with the N atoms above Ga surface atoms) in the 2×2 cell. Alternatively, one can think of this structure as a N-terminated GaN(0001) structure, with 9 of the 12 N dangling bonds (DBs) passivated by H. Within this basic reconstruction, many possible configurations are possible, corresponding to a number of different arrangements of the nitrogen DBs (which are all filled with two electrons). We first carried out calculations addressing the distribution of the DBs over the N atoms in the cell: three DBs all on the same N atom, or two DBs on the same N atom, or each DB on a different N. The structure that we identified to be lowest in energy has the three DBs occurring on three different N atoms. We also investigated the optimal orientation of the DBs: should they all point toward the same $H3$ site, or should the three DBs be parallel? It is the latter arrangement that is most favorable.

In the stable geometry of the NH_3+3NH_2 reconstruction, depicted in Fig. 1, the Ga–N bond lengths in the Ga–NH_2 units are all equal to 1.93 Å, slightly shorter (by 0.03 Å) than Ga–N bonds in the bulk. The Ga–N bond length in the single Ga–NH_3 unit is equal to 2.03 Å, 0.07 Å longer than Ga–N bonds in the bulk. The N–H bonds in the NH_2 units are all very close to 1.03 Å. In the NH_3 unit, one N–H bond is also equal to 1.03 Å, while the other two are slightly longer, at 1.04 Å. For comparison, our calculated N–H bond length in NH_3 is 1.02 Å, very close to the experimental value of 1.01 Å.

The 3Ga–H structure, corresponding to a 3/4 ML coverage of H, is the only stable hydrogen-related structure that has been studied in previous work.[8,11,19] Note that we find the 1/2 ML coverage structure studied in Ref. 19 to be unstable. The three Ga atoms that are bonded to H move outward by 0.09 Å (referenced to the ideal, unrelaxed structure). The remaining Ga atom that is not bonded to H moves into the surface by 0.36 Å, a manifestation of greater tendency toward sp^2 hybridization, as expected for a Ga atom with an empty dangling bond. The Ga–H bond lengths are equal to 1.57 Å.

The NH_3+3Ga–H structure can easily be obtained starting from the 3Ga–H structure by adding one NH_3 unit on top of the one Ga surface atom that is not involved in a Ga–H bond. The three Ga atoms involved in Ga–H bonds now move outward by 0.04 Å, with Ga–H bond lengths equal to 1.60 Å. The Ga atom involved in the Ga–NH_3 bond moves into the surface by 0.13 Å, and the Ga–NH_3 bond length equals 2.05 Å, i.e., 0.09 Å longer than the bulk bond length. The N–H bond lengths are 1.03 Å.

The $NH_3+3Ga–H$ structure is very close in energy to a stoichiometrically equivalent structure, namely $V_{Ga}+6H$, which consists of a Ga vacancy in which all 3 N DBs are saturated with H, plus 3 Ga–H bonds. In this case the three Ga atoms involved in Ga–H bonds move outward by 0.07 Å, with Ga–H bond lengths equal to 1.56 Å. The N–H bond lengths are 1.03 Å.

The remaining structures depicted in Fig. 1 include nitrogen adatoms in the $H3$ position, similar to the N_{ad} reconstruction on the bare surface. In the $N_{ad}–H+Ga–H$ structure, the N adatom sits in an $H3$ position (bonded to three Ga atoms), and a N–H bond is formed on top of this adatom, with a bond length of 1.03 Å. A Ga–H bond is formed on the fourth Ga atom, with a bond length of 1.59 Å. The $N_{ad}–H+NH_2$ structure is very similar to $N_{ad}–H+Ga–H$, but now an NH_2 unit sits on top of the fourth Ga atom. The Ga–N bond length in the $Ga–NH_2$ unit is 1.90 Å, showing a contraction by 0.06 Å with respect to the bulk. The N–H bond lengths in the NH_2 unit are 1.03 Å.

IV. ENERGETICS

Although we made no *a priori* assumptions, we find *a posteriori* that the lowest-energy structures for hydrogenated surfaces all obey *electron counting*. The electron counting rule can be summarized as follows: assuming tetrahedral coordination, a Ga DB contributes 3/4 electron, and a N DB contributes 5/4 electron. For a given surface reconstruction, we count the total number of electrons contributed by Ga and N DBs, as well as by H atoms. Formation of Ga–N, Ga–H, and N–H bonds each requires two electrons; any remaining electrons then need to be accommodated in DBs. Nitrogen DBs have valence-band character; their electronic level is close to the valence-band maximum,[7] and they prefer to be *filled*. Gallium DBs, on the other hand, are close to the conduction band in energy, and prefer to be *empty*. Electron counting is satisfied if the total number of electrons can be accommodated in bonds and in N DBs, leaving no N DBs empty nor Ga DBs occupied. Indeed, an excess of electrons could only be accommodated by placing them in Ga DBs, which carries a high energy cost. Similarly, a deficit of electrons leads to incomplete filling of N DBs, which is also costly.

Within the assumption of tetrahedral coordination, it is easy to verify that the electron counting rule can only be obeyed for structures that contain a multiple of four surface atoms in the unit cell—hence the preference for 2×2 reconstructions. Note that the electron counting rule is not necessarily satisfied on *bare* GaN surfaces, in the absence of hydrogen.[2]

We found that at $T=0$ hydrogenated surfaces that involve a large number of N–H bonds have significantly lower energies than the bare surfaces.[24] This is because N–H bond formation is very favorable due to the large strength of the N–H bond. In particular, the NH_3+3NH_2 structure is stable over almost the entire range of Ga chemical potentials; with nine N–H bonds in the 2×2 cell, this structure maximizes the number of N–H bonds that can be formed while still obeying the electron counting rule.

The picture completely changes at higher temperatures, particularly those relevant for MOCVD growth. This is not so much due to the vibrational contributions to the free energy from species on the surface; those contributions are only on the order of 0.1 eV. By far the largest contribution to the temperature dependence arises from the large change in the value of the hydrogen chemical potential, i.e., the free energy of the reservoir with which H atoms are exchanged. An inspection of the temperature dependence of μ_H [see Eq. (2)] indeed indicates that at 1300 K (and a pressure of 1 atm) μ_H is 0.98 eV lower than at $T=0$. A lower value of μ_H means that less energy can be gained by taking a H atom out of the reservoir and binding it to the GaN surface; this causes the formation energy of structures that contain a large number of N–H bonds to dramatically increase with temperature. The bottom line is that at high temperatures (e.g., $T=1300$ K, representative of MOCVD growth conditions) the energetically favored reconstructions are entirely different from those at $T=0$. While at low temperature several eV could be gained by forming N–H bonds on the surface, at high temperature the energy difference (per 1×1 cell) between hydrogenated and bare surfaces has been reduced to less than 0.3 eV—with the hydrogen-free Ga_{ad} and $Ga_{bilayer}$ structures actually being favored under Ga-rich conditions.

Since changes in temperature (as well as changes in pressure) can have such dramatic effects on the relative stability of different surface structures, we face the question of how to present the information obtained from our first-principles calculations in such a way as to allow more immediate insight into the stability of various structures, for any temperature or pressure. Given that the calculated formation energies are strongly dependent on these quantities, it is not immediately obvious that this can be accomplished. We have been able to show,[24] however, that this goal can be achieved by constructing a phase diagram with the *chemical potentials* as variables.

Figure 2 depicts such a phase diagram for the GaN(0001) surface, with μ_H and μ_{Ga} as the variables. The diagram shown here was calculated at $T=950$ K, but we have verified that the important qualitative features of the diagram are independent of temperature. For example, the calculated phase boundary between 3Ga–H and $NH_3+3Ga–H$ changes by less than 0.1 eV between $T=0$ and $T=1300$ K. The underlying reason is that the vibrational energy contributions to the free energy are relatively small (and cancel to some extent). Obviously, to obtain precise numbers one can refer back to Eq. (1) and take the detailed temperature contributions into account—but important qualitative information can reliably be obtained from Fig. 2, even at temperatures different from $T=950$ K.

At the bottom of the diagram (low μ_H) we find the structures that dominate when little or no H is present: the N_{ad} structure under N-rich conditions, and the Ga_{ad} and $Ga_{bilayer}$ structures under Ga-rich conditions. At the top of the diagram ($\mu_H=0$) we find the structures that were stable at T

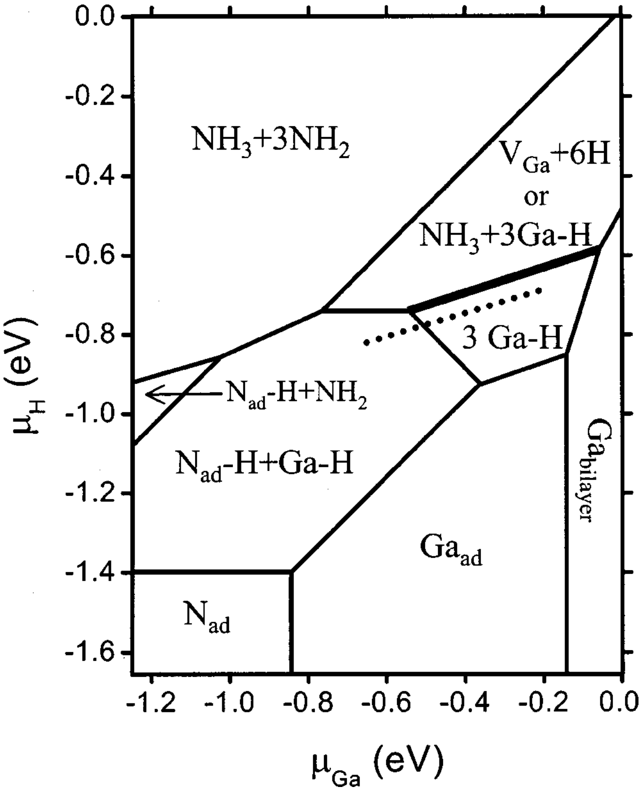

FIG. 2. Phase diagram for the GaN(0001) surface in the presence of hydrogen, as a function of Ga and H chemical potentials. $\mu_H=0$ corresponds to equilibrium with H_2 molecules at $T=0$; $\mu_{Ga}=0$ corresponds to equilibrium with bulk Ga. The NH_3+3Ga–H structure is very close in energy to the stoichiometrically equivalent $V_{Ga}+6H$. Dots indicate experimental data from Ref. 25; within the error bars, these data agree with the calculated NH_3+3Ga–H/3Ga–H phase boundary highlighted by the thicker line.

$=0$. A horizontal line at $\mu_H=-0.98$ eV cuts through the structures that are stable at 1300 K and 1 atm. Figure 2 makes it easy to investigate which structures are stabilized by raising or lowering the pressure or the temperature.

V. COMPARISON WITH EXPERIMENT

As pointed out in Sec. I, direct comparison with experiment is difficult because very few experimental techniques can probe surfaces under the conditions that we are examining here, i.e., at the high temperatures and in the presence of flowing gases relevant for MOCVD growth. The grazing incidence x-ray scattering technique is a fortunate exception. Munkholm *et al.*[25,26] performed *in situ* grazing incidence x-ray scattering on GaN(0001) surfaces in a MOCVD environment. Starting from 2-μm-thick GaN films grown on sapphire by MOCVD, they grew a 30-nm-thick layer at 1000 °C, on which they then performed their search for surface reconstructions. During this search, the sample was held at temperatures up to 1000 °C, and the ammonia pressure $p(NH_3)$ was varied between 2 and 140 Torr. The flow rate of the NH_3/carrier gas mixture was kept constant, with a total pressure of 200 Torr. Results obtained with N_2 as the carrier gas were very similar to those obtained for H_2.

Munkholm *et al.*[25,26] found that the surface equilibrium phase diagram as a function of temperature and ammonia partial pressure shows a transition between two phases: at high temperatures, a 1×1 reconstruction was observed, while at lower temperatures and sufficiently low NH_3 pressures, a different reconstruction was seen, which was identified as $(\sqrt{3}\times2\sqrt{3})R30°$. The phase boundary was established by monitoring the occurrence of either reconstruction at various temperatures and pressures, taking care to achieve equilibrium in each case. From the temperature dependence of $p(NH_3)$ at the transition, an apparent activation energy of 3.0 ± 0.2 eV was extracted, which was interpreted as an activation energy for desorption of the nitrogen species.

A phase transition such as the one observed by Munkholm *et al.* could, *in general*, be related to the *kinetics* of various processes on the surface, including nucleation, diffusion, decomposition, and desorption. The role of these kinetic processes in growth of GaN has been discussed, for instance, by Koleske *et al.*[32] However, we suggest that a simpler interpretation is more appropriate in the present case. First of all, since the phase boundary was obtained from measurements on *equilibrated* surfaces, we feel that the observed activation energy cannot simply be associated with the kinetic barrier for a single process (such as nitrogen desorption). Instead, we will show that the "activation energy" associated with the experimentally established phase boundary can be directly correlated with the energy difference between two surface reconstructions as obtained from our computational study. In fact, we have identified the relevant boundary to be between the 3Ga–H and NH_3+3Ga–H reconstructions. The transition between these reconstructions involves the addition or removal of a single NH_3 molecule per unit cell. No complicated dissociation or nucleation processes are required for such a transition, and the activation energy will not depend on kinetic barriers.

In our phase diagram, the boundary between the 3Ga–H and NH_3+3Ga–H reconstructions is described by the equation $\mu_H=-0.56+\mu_{Ga}/3$ (at 950 K, a temperature in the middle of the experimental range of Ref. 25). The experimental observation that the phase boundary is insensitive to whether H_2 or N_2 is used as the carrier gas allows us to conclude that the transformation between the two observed phases occurs purely through equilibration with NH_3. Note that this equilibrium is really a dynamic equilibrium, where the rate of arrival from a source (the input gases) balances the rate of removal to a sink (the exhaust gas). The fact that the equilibrium is dynamic does not preclude the use of equilibrium concepts such as chemical potentials. The equilibrium with NH_3 implies that $\mu_N+3\mu_H=\mu_{NH_3}$; in other words, in a phase diagram with μ_H and μ_N as the variables, the phase boundary should exhibit a slope of $-1/3$ (or $+1/3$ if μ_{Ga} is chosen as the variable, as in Fig. 2). This already severely restricts the possible phases that could be involved in the experimental observation. For the temperatures and pressures along the experimental phase boundary, the NH_3 chemical potential can be calculated[33] to be equal to -2.28 ± 0.01 eV (referenced to the energy of NH_3 at $T=0$). Using

$\mu_{\mathrm{NH}_3} = -2.28$ eV and $\Delta H_f^{\mathrm{calc}}(\mathrm{NH}_3) = -0.88$ eV we obtain $\mu_{\mathrm{N}} + 3\mu_{\mathrm{H}} = -2.28 - 0.88 = -3.16$ eV, or $\mu_{\mathrm{H}} = -0.64 + \mu_{\mathrm{Ga}}/3$. This expression has been included as a dotted line in Fig. 2. Within the experimental[25] and computational uncertainty, we find good agreement with the calculated $\mathrm{NH}_3 + 3\mathrm{Ga{-}H}/3\mathrm{Ga{-}H}$ phase boundary. The end points of the experimental curve in Fig. 2 correspond to the temperatures and pressures at the limits of the range explored in Ref. 25, assuming H_2 as the carrier gas. These end points also agree with the theoretical diagram, in that at temperatures (or pressures) outside the range reported in Ref. 25 this particular phase boundary should disappear because other reconstructions ($\mathrm{N_{ad}{-}H + Ga{-}H}$ and the Ga bilayer) become more favorable. The experimental observations are therefore consistent with a transition between two structures that differ only in the addition/subtraction of one NH_3 unit in the surface unit cell. This is obvious for the $\mathrm{NH}_3 + 3\mathrm{Ga{-}H}$ structure, which is formed when NH_3 is added to the 3Ga–H structure, but we remind the reader that we found the $V_{\mathrm{Ga}} + 6\mathrm{H}$ structure to be stoichiometrically and energetically equivalent to $\mathrm{NH}_3 + 3\mathrm{Ga{-}H}$.

The 3Ga–H structure is expected to exhibit 1×1 symmetry, since the experiment is not sensitive to H atoms,[25] and disorder (due to different H positions in each 2×2 cell) would reduce the symmetry to 1×1. As to the other reconstruction, we suggest it is unlikely that it would indeed exhibit a $(\sqrt{3} \times 2\sqrt{3})R30°$ symmetry, as proposed in Ref. 25, since such a unit cell would not contain a multiple of four atoms and thus would be highly unfavorable, according to our first-principles results. We note, however, that the actual experimentally observed symmetry in Ref. 25 was $(2\sqrt{3} \times 2\sqrt{3})R30°$. Munkholm *et al.* reduced this to $(\sqrt{3} \times 2\sqrt{3})R30°$ purely to obtain a fit with the smallest number of free parameters. However, a $(2\sqrt{3} \times 2\sqrt{3})R30°$ could not be (and has not been) excluded. Such a reconstruction does contain a multiple of four atoms in the unit cell, in agreement with our conclusions for low-energy structures. Explicit first-principles investigations of structures with 12 atoms in the surface unit cell would be very time consuming, and are also beyond the scope of the present investigations. We suggest, however, that the $\mathrm{NH}_3 + 3\mathrm{Ga{-}H}$ and/or $V_{\mathrm{Ga}} + 6\mathrm{H}$ structures are basic building blocks of the larger reconstruction.

VI. CONCLUSIONS

We have presented first-principles calculations for hydrogenated GaN(0001) surfaces, and outlined a computational approach for obtaining phase diagrams for systems consisting of a surface with an adsorbate. Choosing the chemical potentials as variables significantly simplifies the interpretation of the computed results; this approach produces the phase diagram shown in Fig. 2. Our results served to elucidate experimental observations on this system,[25] illustrating the power of the approach.

A phase diagram such as depicted in Fig. 2 is useful only if the boundary lines are not very sensitive to temperature. We pointed out that this is the case here, the underlying reason being that the vibrational energy contributions to the free energy are relatively small (and cancel to some extent). Hydrogenated GaN is actually a fairly extreme case, with both very high frequencies (N–H bonds, contributing to sizeable vibrational energies) and very low frequencies (torsion modes, contributing to sizeable vibrational entropies). The success of our approach for this extreme case indicates it could be usefully applied to other systems as well.

ACKNOWLEDGMENTS

This work was supported in part by AFOSR (Contract No. F4920-00-C-0019), by the Alexander von Humboldt Foundation, and by the Deutsche Forschungsgemeinschaft (Schwerpunktprojekt "Group-III Nitrides"). The authors are grateful to J. Northrup, M. Scheffler, and O. Brandt for useful discussions and to A. da Rosa for assistance with the initial calculations.

[1] J. E. Jaffe, R. Pandey, and P. Zapol, Phys. Rev. B **53**, 4209 (1996).
[2] J. Neugebauer, T. Zywietz, M. Scheffler, J. E. Northrup, and C. G. Van de Walle, Phys. Rev. Lett. **80**, 3097 (1998).
[3] T. Zywietz, J. Neugebauer, M. Scheffler, J. Northrup, and Chris G. Van de Walle, MRS Internet J. Nitride Semicond. Res. **3**, 26 (1998).
[4] U. Grossner, J. Furthmüller, and F. Bechstedt, Phys. Rev. B **58**, 1722 (1998); Appl. Phys. Lett. **74**, 3851 (1999).
[5] A. Filippetti, V. Fiorentini, G. Cappellini, and A. Bosin, Phys. Rev. B **59**, 8026 (1999).
[6] R. Miotto, A. C. Ferraz, and G. P. Srivastava, Solid State Commun. **115**, 67 (2000).
[7] J. Northrup and J. Neugebauer, Phys. Rev. B **53**, 10477 (1996).
[8] K. Rapcewicz, M. Buongiorno Nardelli, and J. Bernholc, Phys. Rev. B **56**, 12725 (1997).
[9] Q.-K. Xue, Q. Z. Xue, R. Z. Bakhtizin, Y. Hasegawa, I. S. T. Tsong, T. Sakurai, and T. Ohno, Phys. Rev. Lett. **82**, 3074 (1999).
[10] A. R. Smith, R. M. Feenstra, D. W. Greve, J. Neugebauer, and J. E. Northrup, Phys. Rev. Lett. **79**, 3934 (1997).
[11] J. Fritsch, O. F. Sankey, K. E. Schmidt, and J. B. Page, Phys. Rev. B **57**, 15360 (1998).
[12] Z. Yu, L. Buczkowski, N. C. Giles, T. H. Myers, and M. R. Richards-Babb, Appl. Phys. Lett. **69**, 2731 (1996).
[13] Y. Okamoto, S. Hashiguchi, Y. Okada, and M. Kawabe, Jpn. J. Appl. Phys., Part 2 **38**, L230 (1999).
[14] C. Bungaro, K. Rapcewicz, and J. Bernholc, Phys. Rev. B **59**, 9771 (1999).
[15] S. Picozzi, A. Continenza, and A. J. Freeman, Phys. Rev. B **59**, 1609 (1999).
[16] T. Zywietz, J. Neugebauer, and M. Scheffler, Appl. Phys. Lett. **74**, 1695 (1999).
[17] T. Zywietz, J. Neugebauer, and M. Scheffler, Appl. Phys. Lett. **73**, 487 (1998).
[18] J. E. Northrup, R. Di Felice, and J. Neugebauer, Phys. Rev. B **56**, 4325 (1997).
[19] J. Elsner, M. Haugk, G. Jungnickel, and Th. Frauenheim, Solid State Commun. **106**, 739 (1998).
[20] M. M. Sung, J. Ahn, V. Bykov, J. W. Rabalais, D. D. Koleske, and A. E. Wickenden, Phys. Rev. B **54**, 14652 (1996).
[21] C.-M. Chiang, S. M. Gates, A. Bensaoula, and J. A. Schultz, Chem. Phys. Lett. **246**, 275 (1995).
[22] R. Shekhar and K. F. Jensen, Surf. Sci. **381**, L581 (1997).
[23] V. J. Bellitto, B. D. Thoms, D. D. Koleske, A. E. Wickenden, and R. L. Henry, Surf. Sci. **430**, 80 (1990); Phys. Rev. B **60**, 4816 (1999); **60**, 4821 (1999).
[24] C. G. Van de Walle and J. Neugebauer, Phys. Rev. Lett. **88**, 066103 (2002).

[25] A. Munkholm, G. B. Stephenson, J. A. Eastman, C. Thompson, P. Fini, J. S. Speck, O. Auciello, P. H. Fuoss, and S. P. DenBaars, Phys. Rev. Lett. **83**, 741 (1999).
[26] A. Munkholm, C. Thompson, G. B. Stephenson, J. A. Eastman, O. Auciello, P. Fini, J. S. Speck, and S. P. DenBaars, Physica B **283**, 217 (2000).
[27] P. Hohenberg and W. Kohn, Phys. Rev. **136**, B864 (1964); W. Kohn and L. J. Sham, Phys. Rev. **140**, A1133 (1965).
[28] M. Bockstedte, A. Kley, J. Neugebauer, and M. Scheffler, Comput. Phys. Commun. **107**, 187 (1997).
[29] H. J. Monkhorst and J. D. Pack, Phys. Rev. B **13**, 5188 (1976).
[30] *CRC Handbook of Chemistry and Physics*, 73rd ed., edited by David R. Lide (Chemical Rubber Corp., Boca Raton, FL, 1992), pp. 5–18.
[31] J. E. Northrup, J. Neugebauer, R. M. Feenstra, and A. R. Smith, Phys. Rev. B **61**, 9932 (2000).
[32] D. D. Koleske, A. E. Wickenden, R. L. Henry, W. J. DeSisto, and R. J. Gorman, J. Appl. Phys. **84**, 1998 (1998).
[33] D. R. Stull and H. Prophet, *JANAF Thermochemical Tables*, 2nd ed., U.S. National Bureau of Standards NSRDS-NBS 37 (U.S. GPO, Washington, D.C., 1971).